

In Situ Mechanistic Investigation at the Liquid/Solid Interface by Attenuated Total Reflectance FTIR: Ethanol Photo-Oxidation over Pristine and Platinized TiO₂ (P25)

Dangguo Gong,^{†,‡} Vishnu Priya Subramaniam,^{†,‡} James G. Highfield,^{*,†} Yuxin Tang,[†] Yuekun Lai,^{†,§} and Zhong Chen^{*,†}

[†]School of Materials Science and Engineering, Nanyang Technological University, 50 Nanyang Avenue, Singapore 639798, Singapore

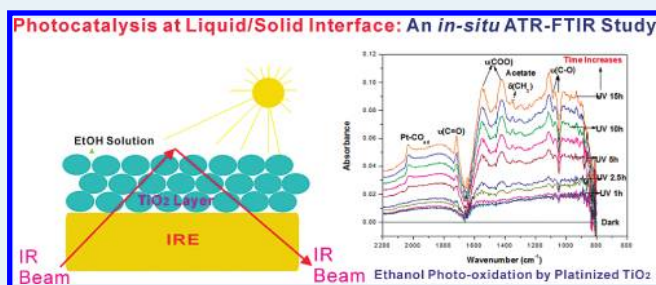
[‡]Heterogeneous Catalysis, Institute of Chemical & Engineering Sciences, 1 Pesek Road, Singapore 627833, Singapore

[§]State Key Laboratory of Physical Chemistry of Solid Surfaces and Department of Chemistry, College of Chemistry and Chemical Engineering, Xiamen University, Xiamen 361005, China

S Supporting Information

ABSTRACT: There is growing interest in applying photocatalysis to help solve both the energy crisis and effectively combat environmental contamination. However, it is difficult to investigate photocatalytic reactions at the liquid/solid interface to unravel the reaction mechanism by conventional (ex situ) surface analytical techniques. In this study, Attenuated Total Reflectance-FTIR spectroscopy, adapted for optical pumping, was used to observe in situ the surface of TiO₂ (Degussa P25, in both pristine and platinized forms) during photocatalytic oxidation of ethanol aqueous solution. It shows the feasibility to investigate not only the reaction pathway and the rate-determining step, but also the change in state of the catalyst under working conditions. During ethanol photo-oxidation over pristine TiO₂, band gap excitation caused the progressive accumulation of trapped electrons, as recognized by their characteristic quasi-continuum absorption, implying that photoreduction does not proceed at a significant rate under these conditions. Consistent with this view, only weak infrared features due to adsorbed intermediates were observed. Over platinized TiO₂, the noble metal nanodeposits promote photodehydrogenation and photoactivation of dioxygen. In addition to observing strong bands diagnostic of various intermediates, the presence or absence of a band around 2050 cm⁻¹, typical of Pt-CO_{ad}, served as a valuable spectroscopic marker of the instantaneous availability of the chemical oxidant. As such, mechanistic parallels were found between photoreforming (with H₂ generation) and photo-oxidation (to acetate), with acetaldehyde being a common intermediate in both processes. The rate-determining step in ethanol mineralization was found to be photodecomposition of adsorbed acetate.

KEYWORDS: in situ, ATR-FTIR, photocatalysis, photo-oxidation, ethanol



1. INTRODUCTION

Interest in photocatalysis driven by solar light has risen greatly over the past two decades. It offers excellent prospects to help solve both the energy crisis (by generating renewable hydrogen endergonically, even from water), and effectively combat environmental pollution by gas- and liquid (aqueous)-phase photo-oxidation, a photoassisted downhill process.^{1–4} Elucidation of reaction mechanism is vital to gain insight into the current limitations of photocatalysts and to improve their efficiency and stability by rational design. However, more in situ studies at the photocatalyst surface under working conditions are needed to unravel the mechanistic detail.

Modern vibrational infrared (IR) spectrometers based on Fourier-Transform (FT) methods have made FTIR a very powerful and versatile tool in fundamental and applied studies of heterogeneous catalysts and reactions at their surfaces. However, while pressed-disk transmission and Diffuse Reflectance

(DRIFT) techniques for in situ studies of powdered samples at the gas/solid interface have continued to dominate research over the past two decades, there is a growing need to extend investigations to catalysts immersed in liquids as reactants and/or solvents. The optical sampling variant known as Attenuated Total Reflectance (ATR), which greatly reduces interference from solvent absorption due to shallow penetration by the evanescent IR probe wave, is now emerging as the tool of choice to derive qualitative and semiquantitative information at the liquid/solid interface.^{5,6} Unusual mediating effects of liquid water on the reactivity of adsorbed species have also been claimed in a recent review of this technique.⁷ In photocatalysis, Nakato et al.^{8,9} have identified the surface peroxo species as the primary intermediate

Received: February 6, 2011

Revised: April 30, 2011

Published: June 01, 2011

of O₂ photoreduction using in situ ATR-FTIR. However, for reasons of instrumental sensitivity, many early studies in environmental photocatalysis at the liquid/solid interface have been restricted to reactants with strong IR chromophores, that is, oxalic acid,^{10–12} malonic acid,¹³ and other dicarboxylic acids,¹⁴ because of the typical low levels at which these are found as natural pollutants. Bahnemann et al.^{10–12} found that oxalate adopts two bidentate conformations: A (carbon–carbon σ bond parallel to the surface) and B (carbon–carbon σ bond perpendicular to the surface) on anatase TiO₂ surface under dark conditions. Typically, species A predominates during and after UV illumination, suggesting that species B is more easily attacked and degraded by photogenerated radicals. However, the absence of identifiable intermediates made further mechanistic insight difficult in their study. Elsewhere, Bürgi et al. found that oxalate is a major intermediate in the photomineralization of malonate.^{13,14} Succinate is degraded to malonate initially, which is then further degraded to oxalate¹⁴ in what appears to be a stepwise shortening of the hydrocarbon chain by the photo-Kolbe reaction. While changes in the electronic state of TiO₂ induced by UV illumination using in situ ATR-FTIR has just been reported,¹⁵ to the best of our knowledge its correlation with photocatalytic activity and the effect of metallization, as described herein, is new.

Interest in this Laboratory centers on the photocatalytic reforming of simple alcohols like methanol¹⁶ and ethanol.^{17–19} Such compounds, if derived from biomass, may be considered as high-density storage forms of renewable hydrogen. While DRIFTS (vapor/solid) investigations of ethanol photo-oxidation have been reported,^{20–22} adventitious oxidation of ethanol in the condensed (dilute aqueous) phase is of more concern in practice, since most bioethanol is worked up from fermentation broth in just such a form.

In the present work, we apply in situ ATR-FTIR spectroscopy to study the photo-oxidation of dilute aqueous ethanol, including direct tests on probable intermediates, acetaldehyde and acetic acid, over pristine and platinumized Degussa P25 TiO₂. As compared to pure TiO₂, which was barely active, simultaneously accumulating electronic charge, platinumization enhanced the photo-reduction process by acting as an electron “sink” and more effectively activating dioxygen for mineralization. Ethanol is oxidized (photodehydrogenated) initially to acetaldehyde, and then to acetic acid. Evidence for C–C bond cleavage is also shown by the appearance of metal-adsorbed CO. However, the mineralization of acetic acid (as sorbed acetate) was very slow, suggesting it is the rate-determining step (RDS) in ethanol photomineralization.

2. EXPERIMENTAL SECTION

2.1. Materials. Pristine titanium dioxide used throughout this study was Degussa P25 TiO₂, which is composed of about 80% anatase phase and 20% rutile phase. Its primary particle size is about 30 nm, and the Brunauer–Emmett–Teller (BET) surface area is about 50 m²·g⁻¹. Platinumized P25 TiO₂ was prepared through a photoreductive deposition process. Suitable amounts of TiO₂ and H₂PtCl₆, to arrive at a nominal loading of 0.5 wt % Pt, were added to a mixture of deionized water and methanol in a volume ratio of 5:1 and illuminated by a 450 W Xe lamp (total flux \approx 200 mW·cm⁻²) for 2 h. The suspension was isolated by centrifugation, washed 3 times in deionized water, and dried in an oven at 70 °C overnight. TEM confirmed that the Pt was homogeneously dispersed on the TiO₂ in a fairly narrow particle diameter range of 2–3 nm (see Supporting Information, Figure S1).

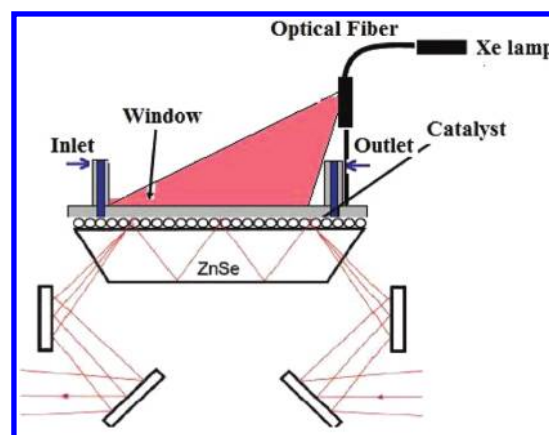


Figure 1. Scheme of the ATR-FTIR set up.

All other chemicals were bought from Sigma-Aldrich and used directly without any further purification.

2.2. Equipment and Methodology. The scheme of the ATR setup is shown in Figure 1. It consists of a Pike multiple internal reflection accessory, coupled to a 2 mL internal volume flow-through cell containing an optically dense crystal (ZnSe unless otherwise indicated) as the internal reflection element (IRE) and a UV transparent fused silica window as the top plate. A crystal (dimensions = 80 × 10 × 4 mm) with a 45° entrance angle was chosen as it allows 10 infrared beam deflections for progressive absorption and good sensitivity. The optical fiber bundle was a 1 m long high-quality quartz variant (Oriell 77539), actually designed for coupling to a monochromator slit, but here used in reverse. This provided a slightly diverging rectangular output from an Oriell 150 W Xe DC short arc lamp, permitting illumination of roughly 80% of the sample area by careful adjustment of the fiber mounting clamp. One disadvantage of this set up is that the ATR collects some information from the small unilluminated sample area at each end of the crystal, potentially lowering the reactive “contrast” between light and dark experiments.

The ATR accessory was mounted kinematically in the front sample compartment of the Digilab Excalibur FTS-3000 FTIR spectrometer (Varian Inc.). It was supplied with liquid reactants from a circulating pump at a typical flow rate of 1–5 mL·min⁻¹. The ethanol and acetaldehyde aqueous solutions used in this study, respectively 0.86 and 0.89 M, were close to neutral pH. The acetic acid solution (1 mM) was rendered less acidic (pH raised to \sim 5 with NaOH) to protect the IRE from corrosion.

Deionized (DI) water was first circulated through the cell and a background spectrum was taken under dark (reference) conditions. After that, the aqueous solution of reactant, prepurged in air, was supplied into the cell, and its IR bands were tracked. Once these reached steady-state, the pump was stopped, and then the lamp was turned on. In other words, the reaction was studied in static conditions without additional O₂ supply. Time-resolved IR spectra were collected every two minutes (120 coadded scans per spectrum to improve signal-to-noise) over the range 4000–1000 cm⁻¹ at 4 cm⁻¹ resolution using the *kinetics* mode of the Resolutions Pro 4a software supplied with the spectrometer.

2.3. Thin Film Preparation. ATR-FTIR is a type of internal reflection spectroscopy in which the sample is placed in close contact with IRE of high refractive index. Powdered catalysts must be immobilized as a homogeneous thin film onto the IRE (ZnSe crystal in these experiments). Powder photocatalysts were

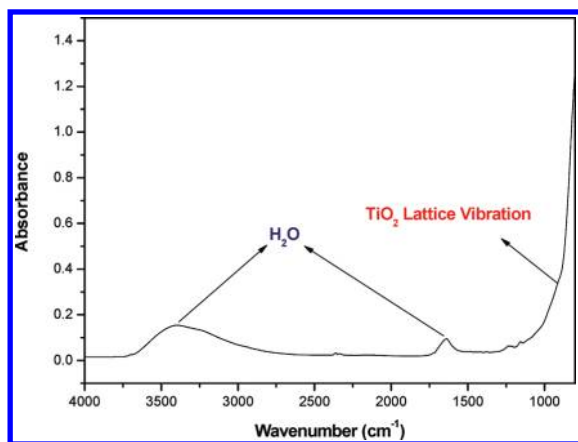


Figure 2. ATR-FTIR spectrum of TiO₂ thin film (density $\sim 5 \text{ mg} \cdot \text{cm}^{-2}$) deposited on ZnSe crystal (spectral background obtained from the clean dry crystal).

first suspended in deionized water at a concentration of $10 \text{ mg} \cdot \text{mL}^{-1}$. The suspension was then treated in an ultrasonic bath for 30 min, and $400 \mu\text{L}$ of this suspension was gently and evenly spread on the ZnSe crystal and left to dry overnight at room temperature. The coverage of the final dry layer of TiO₂ particles thus obtained was about $5 \text{ mg} \cdot \text{cm}^{-2}$ and the layer appeared homogeneous under visual inspection. The thickness of this layer was estimated as typically around $4 \mu\text{m}$ based on the bulk density of P25 TiO₂.

Although the refractive index of bulk TiO₂ ($n = 2.6$ for anatase) is slightly larger than that of ZnSe ($n = 2.4$), the effective n of the porous particle film of TiO₂ in contact with water ($n = 1.33$) could be effectively reduced to below 1.7.⁶ The penetration depth of the evanescent wave into the TiO₂ layer is estimated to be less than $1.4 \mu\text{m}$ at 1640 cm^{-1} (ZnSe/H₂O system),⁵ so most of the information should be from this layer.

The IR spectrum of a typical deposited layer of TiO₂ is shown in Figure 2. The pronounced absorption below 1000 cm^{-1} is characteristic of the intense TiO₂ lattice phonon. This was used as a “gauge” in preliminary work to arrive at a suitable layer thickness ($4\text{--}5 \mu\text{m}$) with acceptably high spectral contrast.

3. RESULTS AND DISCUSSION

3.1. Adsorption from Aqueous Ethanol on Thin-Layers of Pristine and Platinized P25 TiO₂ under Dark. In the first of a series of control experiments, Figure 3 shows spectral changes on the P25 TiO₂ surface when 0.86 M EtOH solution (O₂-free) was circulated into the ATR cell in the dark after preconditioning in DI water. Displacement of water from the TiO₂ surface is indicated by two broad negative H₂O bands, respectively at $3600\text{--}3000 \text{ cm}^{-1}$ (ν_{OH}) and $1700\text{--}1500 \text{ cm}^{-1}$ (δ_{OH}), while positive bands emerged characteristic of ethanol around $3000\text{--}2800$, $1400\text{--}1300$, and $1100\text{--}1000 \text{ cm}^{-1}$ (band assignments as indicated in Figure 3). A similar competition between alcohol and water for adsorption sites on P25 TiO₂ has already been seen for methanol by DRIFTS in this laboratory.¹⁵ Various reports have shown that simple monobasic alcohols adsorb on anatase and rutile surfaces in both molecular and heterolytically dissociated forms.^{23–25} For ethanol, dissociation results in sorbed ethoxide groups atop a Lewis acidic Ti⁴⁺ center (monodentate) or between two Ti⁴⁺ centers (bidentate), while the H from the alcohol associates with a neighboring basic surface O to form an OH group.^{23,25} The

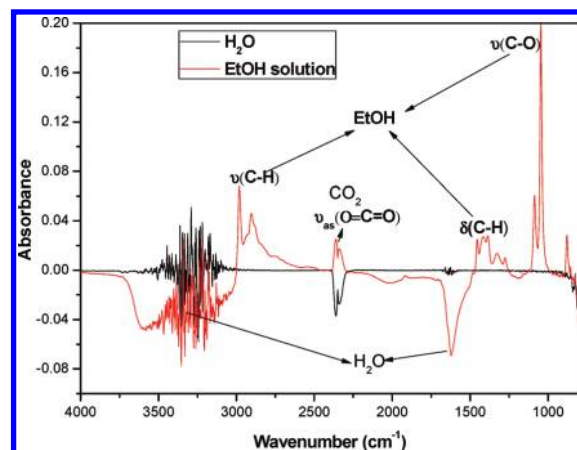


Figure 3. ATR-FTIR spectra after adsorption of aqueous ethanol (red) on P25 TiO₂. The background spectrum (black) was obtained by pre-immersion in DI water.

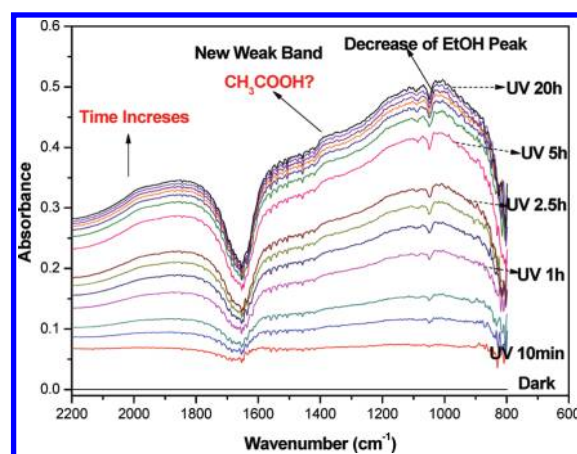


Figure 4. ATR-FTIR difference spectra recorded during photo-oxidation of ethanol over P25 TiO₂ (dark-subtracted).

possibility of detecting ethanolic species on the metal component is extremely low in view of the small Pt loading and the relatively weak interaction. Indeed, very little difference can be seen between spectra taken either in the presence or absence of the photocatalyst layer (see Supporting Information, Figure S2). Thus, the ATR-FTIR setup in this case (ethanol in the dark) samples mainly bulk species. The small change in absorption at 2350 cm^{-1} is an instrumental artifact associated with the FTIR spectrometer. Slow and periodic microchanges in the compressed dry air purge quality protecting the KBr beamsplitter result in a slightly varying level of gaseous CO₂.

3.2. Ethanol Photo-Oxidation over Pristine TiO₂. Figure 4 shows the ATR-FTIR difference spectra recorded during the photo-oxidation of EtOH over pristine P25 TiO₂ (raw spectra: see Supporting Information, Figure S3). The most striking feature here is the initially rapid upward shift in the baseline, evidently more pronounced in the low-wavenumber range, peaking at around 1000 cm^{-1} . There is also a progressive and contemporaneous weakening of the deformation band due to adsorbed water at $\sim 1625 \text{ cm}^{-1}$. Coincidentally, we have just become aware of independent ATR-FTIR studies reporting very similar features for TiO₂ in aqueous oxalate environment.¹⁵ Whereas these

authors attribute the water loss to hole-induced photodissociation into surface OH groups, we think this is not very likely in the presence of ethanol, which is by far the superior hole scavenger. However, there is another key difference in reaction conditions. Whereas in Figure 4 the background absorption (and water loss) develops under oxygenated conditions, Savory et al. worked under anaerobic conditions and effected rapid elimination of these spectral features by introduction of air. This sensitivity to O₂, which can ionosorb as superoxide (O₂⁻) and/or act as a recombination center, is consistent with previous literature. Pioneering DRIFTS studies by Hoffmann et al.^{26,27} are the original source of the continuum mid-IR absorption seen over O₂-free hydroxylated TiO₂, which they convincingly demonstrated was associated with photogenerated electrons filling (energetically) deep or shallow surface traps. Prior to this work, pump–probe UV–vis–NIR photoacoustic spectroscopy was used to study the analogous long-lived and reversible photochromism in P25 TiO₂ (small polaron absorption, peaking in the near IR region), again illustrating the importance of having moist O₂-free conditions to best visualize this feature.^{28,29} Otherwise, there are only minor spectral changes in Figure 4, suggesting that photomineralization of aqueous ethanol is severely impaired over pure TiO₂. There is slow conversion of EtOH, as indicated by the gradual appearance of negative peaks around 1050 cm⁻¹ due to the C–O stretch. However, the decrease in integrated area of this band suggests just a few percent conversion after illumination for more than 20 h. Acetaldehyde and acetic acid are both known intermediates of ethanol photo-oxidation in the vapor phase.^{20–22,30,31} However, the ν_{C=O} band of acetaldehyde, expected at ~1715 cm⁻¹, is obscured by the relatively strong negative δ_{HOH} band at ~1630 cm⁻¹. Similarly, while there is a weak development of broad features in the range 1500–1300 cm⁻¹, where the doublet due to adsorbed acetate would be expected, the strong background absorption renders them insufficiently defined for any confident assignment. Accordingly, little or no difference was seen in ATR-FTIR between aerated and deaerated solution. It remains unclear why the background absorption develops even in an aerated ethanolic solution, although a tentative explanation is proffered later (*vide infra*).

3.2. Ethanol Photo-Oxidation over Platinized TiO₂. From control tests under both dark/aerated and UV/deaerated (photo-reforming) conditions, little or no change was observed in the ATR-FTIR spectra when aqueous ethanol was equilibrated over a deposited layer of 0.5 wt % Pt/TiO₂ during 15–20 h (see Supporting Information, Figures S4 and S5). Figure 5 shows the ATR-FTIR difference spectra recorded under photo-oxidizing (UV/aerated) conditions (raw spectra: see Supporting Information, Figure S6). The first substantial difference with pristine TiO₂ is the only slight build-up in background absorption over many hours. In addition, absorption bands characteristic of acetaldehyde (carbonyl stretch, ν_{C=O}, at 1715 cm⁻¹) and acetate (asymmetric and symmetric stretch of the carboxylate moiety (ν_{OCO}) at 1550 and 1415 cm⁻¹, respectively), were seen already within the first few hours of illumination and continued to grow overnight. The identities of these intermediates were confirmed in separate experiments by their direct contact with the fresh catalyst, as described later (*vide infra*).

The most likely sequence is that EtOH in aqueous solution over the platinized sample first undergoes photodehydrogenation (PDH) to acetaldehyde, which is in turn oxidized to acetic acid. According to Pichat,³² the production of aldehydes from alcohols over Pt/TiO₂ involves a combination of dissociative

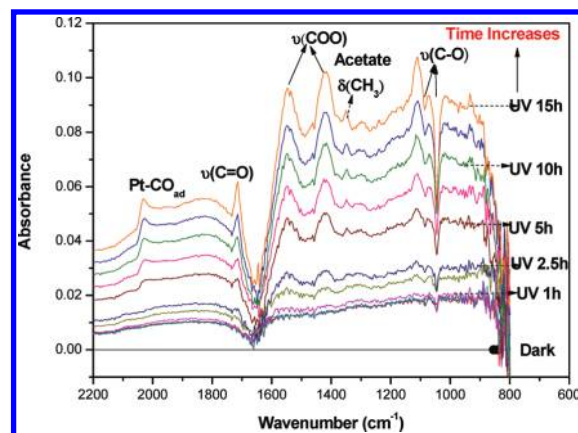
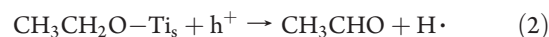
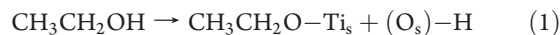
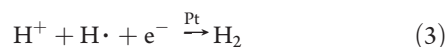


Figure 5. ATR-FTIR difference spectra recorded during photo-oxidation of EtOH over 0.5 wt % Pt/P25 TiO₂.

adsorption in the dark and H abstraction from the adsorbed alkoxy group by a photogenerated hole, as shown schematically for ethanol in eqs 1 and 2:



where Ti_s and O_s are surface ions (formal charges omitted for clarity). PDH is completed by proton discharge and H atom recombination over Pt:



The summation of eqs 1–3 corresponds to ethanol PDH:



which, while efficient ($\Phi \approx 0.5$), is also endergonic (thermodynamically uphill),³³ with an enthalpy increase of 86 kJ·mol⁻¹. Under the static, ambient (equilibrium) conditions applied here, there is a strong likelihood of thermodynamic control, that is, back-reaction between acetaldehyde and hydrogen. This would explain why no clear evidence was seen for acetaldehyde in the photoreforming control test (Supporting Information, Figure S5). Nevertheless, extended illumination eventually gave rise to very slight bubbling, which was identified as H₂ gas by MS in separate experiments. Thus, evidence of more acetaldehyde production under photo-oxidative conditions can only be rationalized as “oxidative dehydrogenation”, that is, any H atoms are rapidly scavenged by dioxygen to produce water.

Extended illumination gradually gave rise to an additional band around 2050 cm⁻¹, which is characteristic of CO adsorbed on Pt in the “on-top” position.^{34–37} It appeared initially at about 2030 cm⁻¹ but progressively shifted to higher frequency because of the coverage-dependent dipolar coupling effect. Identical features have already been observed over Pt/TiO₂ by DRIFTS during photoreforming of methanol vapor.¹⁶ However, it is a surprising observation insofar as, from our previous work on methanol photoreforming, adsorbed CO on Pt was extremely reactive with ambient air even in the dark. Furthermore, previous independent ATR-FTIR studies of CO oxidation over Pt/Al₂O₃ emphasize that the liquid environment has a dramatic influence on the rate, being accelerated in pure water,^{38,39} but markedly hindered in ethanol,⁴⁰ as compared to the gas-phase. So although

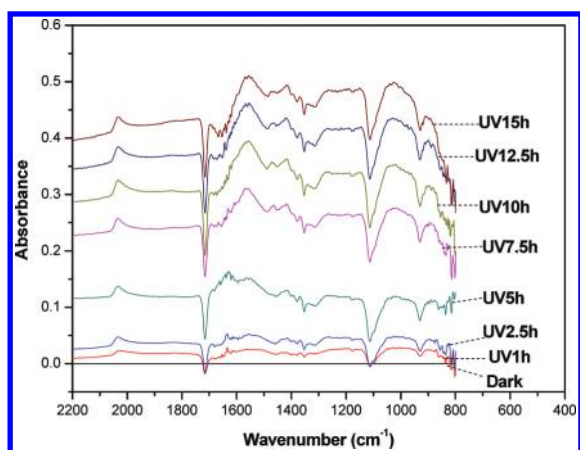


Figure 6. ATR-FTIR difference spectra recorded during photo-oxidation of acetaldehyde over 0.5% Pt/P25 TiO₂.

the cause of the growth of the Pt-CO_{ad} species is unclear at this stage, it inevitably raises concerns as to the maintenance of O₂ supply over the entire experiment. One potential source of CO is decarbonylation of acetaldehyde:



Although it is difficult to identify products in the gas phase by the ATR technique, CH₄ has been detected by in situ DRIFTS during ethanol photoreforming at elevated temperature. This will be discussed elsewhere.⁴¹

Despite the aforementioned concerns, the acetate bands continued to grow alongside Pt-CO_{ad}, indicating that acetic acid is, at least partially, derived from the Cannizzaro disproportionation, which does not formally require dioxygen, water acting as oxidant instead:



This is the analogous process identified as the source of formate from methanol in photoreforming.¹⁶ Early studies of ethanol reforming in thermal heterogeneous catalysis led to a similar conclusion, although temperatures close to 100 °C were required to develop adsorbed acetate bands from the aldehyde over a Co/Cu/MgO catalyst.¹⁸

3.3. Acetaldehyde and Acetic Acid Photo-Oxidation over Platinized TiO₂. Having verified the identities of two key intermediates in ethanol conversion, namely, acetaldehyde and acetic acid, their independent and direct photo-oxidation on platinized TiO₂ was also of interest to build up a plausible mechanistic scheme. Figure 6 shows ATR-FTIR difference spectra recorded during the photo-oxidation of acetaldehyde over platinized TiO₂ (raw spectra: Supporting Information, Figure S7). Consumption of the aldehyde is seen most clearly as the progressive weakening (to more negative values) of the diagnostic carbonyl stretch, $\nu_{\text{C=O}}$, at 1720 cm⁻¹. The gradual appearance of Pt-CO_{ad} proves that the aldehyde is indeed one source of CO. However, unless conditions are well-controlled and rates carefully compared, this does not rule out an additional route to CO from ethanol in which the C–C bond is cleaved *before* dehydrogenation.^{42,43} To evaluate this, Figure 7 compares the growth curves for Pt-CO_{ad} derived from the aldehyde (Figure 6) and from the alcohol (Figure 5) under otherwise equivalent conditions. These show that CO is generated immediately and initially faster from acetaldehyde. The delay in appearance of

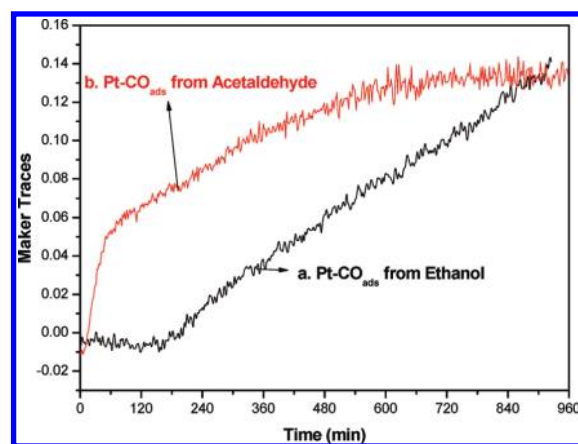


Figure 7. Growth of Pt-CO_{ads} as observed during photo-oxidation: (a) from 0.86 M ethanol (black); (b) from 0.89 M acetaldehyde (red).

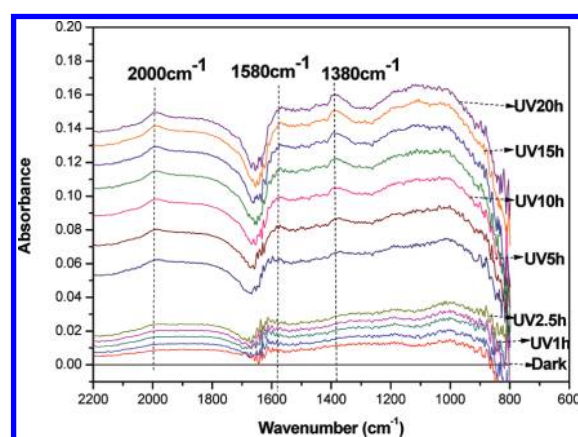


Figure 8. ATR-FTIR difference spectra recorded during photo-oxidation of 1 mM acetic acid over 0.5 wt % Pt/P25 TiO₂.

CO from ethanol can be interpreted as a sensitivity issue, that is, the time required for sufficient build-up of aldehyde level, it being mechanistically the most immediate, and apparently the sole, source of CO. Decarbonylation of acetaldehyde is evidently *photo-activated* as no adsorbed CO band developed over several hours in the dark prior to illumination.

Figure 6 also shows that the bands of acetate (asymmetric and symmetric stretch of the carboxylate moiety, $\nu_{(\text{OCO})}$, around 1550 and 1415 cm⁻¹, respectively) grew with time, confirming that acetaldehyde was gradually converted to acetic acid in a parallel process to decarbonylation.

The direct photo-oxidation of acetic acid was also carried out under the same conditions, and ATR-FTIR difference spectra are shown in Figure 8 (raw spectra: Supporting Information, Figure S8). A 1 mM acetic acid solution was illuminated for more than 15 h, but the diagnostic bands of acetic acid did not even become weaker. Furthermore, the background absorption remained low, suggesting that the acetate species is not an efficient hole scavenger, unlike the analogous (C₂) alcohol, probably because of the absence of sufficiently photolabile H.^{44,45} A weak band of Pt-CO_{ad} appeared eventually at ~2000 cm⁻¹, similar to those observed from ethanol and acetaldehyde, suggestive of decarbonylation:



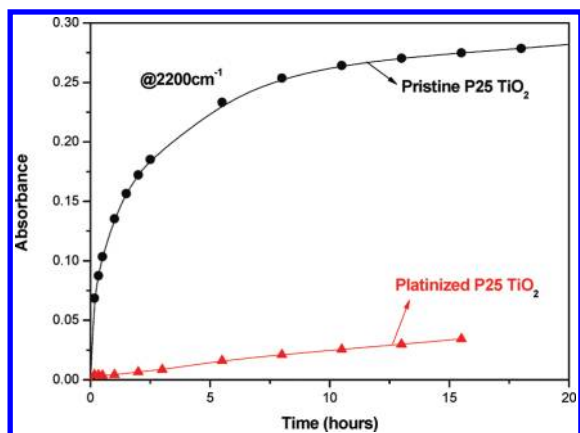


Figure 9. Growth curves for continuum absorption (at 2200 cm^{-1}) during photo-oxidation of aqueous ethanol over pristine and platinumized TiO_2 .

but a putative methoxy group as product would be difficult to distinguish from acetate because of near coincidence in the C–H stretching and bending vibrations of the methyl group common to both.

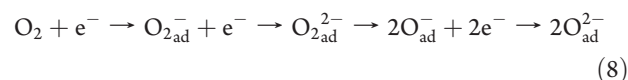
Acetate decarbonylation is rather surprising since CO_2 is a more likely product via simple photohole-stimulated decarboxylation, or possibly along with CH_4 and C_2H_6 via a Photo-Kolbe coupling mechanism.⁴⁶ An additional indirect test for any CO_2 was made. In situ production was simulated by sparging CO_2 through liquid water, with the aim of forming a bulk bicarbonate species readily detectable by ATR-FTIR. The spectral signature (see Supporting Information, Figure S9), against both pure water and the platinumized catalyst is consistent, showing two bands of similar intensity close to 1575 and 1325 cm^{-1} , assigned as the asymmetric and symmetric stretch of the bicarbonate moiety.¹⁴ The other two weak bands growing at 1580 cm^{-1} and 1380 cm^{-1} in Figure 8 can be tentatively assigned to adsorbed carbonate species.⁴⁷

Evidently, the photomineralization of acetic acid is very slow indeed and the integrated areas of the acetate bands in the raw spectra (see Supporting Information, Figure S8) even increased slightly, and unexpectedly, under illumination, similar to what Bahnemann et al.¹¹ reported for oxalate on TiO_2 during UV illumination. The increase of acetate adsorption here is more likely due to the photoinduced desorption of water from the TiO_2 surface, as indicated by the negative band around 1630 cm^{-1} under illumination. Thus, further acetate adsorption becomes possible. Nevertheless, these slight changes do not obscure or fully explain the growth of bands (and the 1380 cm^{-1} band in particular) in the difference spectra which can be taken as evidence for adsorbed carbonate.

The underlying difficulty in activating adsorbed acetate is not yet clear, but it is not altogether surprising since it has also been identified as the RDS by various groups studying ethanol reforming in thermal heterogeneous catalysis.^{18,48–50} It may be that it is intrinsically stable and/or that its strong adsorption on TiO_2 prevents access by the oxidant in sorbed form. In any event, the evidence suggests that the RDS in ethanol photo-oxidation over platinumized TiO_2 is the activation and mineralization of acetic acid.

3.4. Photocatalyst Charging under Band Gap Excitation and Its Correlation with Photoactivity. As shown in Figure 9, the continuum growth or “charging” curve in pristine TiO_2

appears almost exponential with an asymptote, consistent with Hoffmann’s view of progressive filling of a fixed number of electron trap states.^{22,23} The build-up of long-lived electronic charge confirms efficient hole scavenging by ethanol, as expected. However, it also suggests that the complementary process to sustain a photo-oxidation cycle, namely, activation of molecular oxygen via ionosorption to form adsorbed superoxide, peroxide, (a 4 electron transfer process overall):



occurs only slowly; a situation that cannot be sustained indefinitely. The accumulation of excess negative charge on the catalyst surface will impede hole-induced chemistry by progressively increasing the probability of electron/hole recombination. Consistent with this view, TiO_2 per se appears a poor catalyst for ethanol photo-oxidation. In contrast (see Figure 9), the presence of Pt suppresses dramatically the charging effect in TiO_2 , and at the same time promotes much higher photoactivity. Pt should act as an efficient electron sink and mediator regardless of the identity of the electron acceptor(s) present at the surface. For good photo-oxidation activity, O_2 must compete with H^+ and H^* for adsorption sites on Pt (see eq 3). Provided there is a good supply of oxidant, there is little reason to doubt this since the kinetics of Pt-catalyzed H_2 oxidation (to water) are well-known.⁵¹ Indeed, this has been indirectly verified here in the fact that O_2 promotes aldehyde production. Furthermore, Pt remains the best cathode material for the O_2 electro-reduction reaction (ORR) in PEM fuel cells.^{52,53} Any aldehyde-derived CO which becomes bound to Pt should also be readily converted to CO_2 , but the stable CH_4 coproduct is undesirable as it is a potent greenhouse gas. For more complete mineralization of the organic carbon, the preactivated oxidant must migrate or “spill over” to intermediate(s) with the C–C bond still intact, that is, adsorbed ethoxy, aldehyde, or a derivative species like the acetyl radical ($\text{CH}_3\text{CO}\bullet$), all of which will be bound predominantly to the oxide surface. Evidence for such oxygen spillover has been reported.⁵⁴ Although dioxygen can be ionosorbed directly on TiO_2 as superoxide ($\text{O}_2^{\text{ad}-}$), there is little evidence for this on the pristine TiO_2 surface as studied here, otherwise it should have suppressed the growth of the IR continuum, notwithstanding any hindrance by the ethanol component (vide ultra). Additional electron trapping to form the peroxy species ($\text{O}_2^{\text{ad}2-}$), and/or irreversible dissociation into more highly activated $\text{O}_{\text{ad}}^{\text{ad}-}$ species (see eq 8) seems much more probable on Pt.^{51,52} Indeed, evidence for multiple electron transfer at Pt, for example, direct formation of peroxide, provides the only plausible explanation for sustained photo-oxidation of organic compounds over Pt/ WO_3 . In this case, the reduction potential at the conduction band edge of the oxide is insufficiently negative to generate superoxide in a single electron transfer step.⁵⁵ This is also a topical issue in view of growing interest in the direct synthesis of H_2O_2 from H_2 and O_2 .⁵⁶

4. CONCLUSION

The present work demonstrates the feasibility of in situ ATR-FTIR spectroscopy, adapted for optical pumping, to investigate not only the reaction pathway but also the change in electronic state of the photocatalyst under *operando* conditions and its relation to activity.

As model reactions, the photo-oxidation of ethanol, acetaldehyde, and acetic acid have been studied. These show that ethanol photo-oxidation over pristine TiO₂ is quite slow. Band-gap excitation causes the accumulation of free electrons with their associated quasi-continuum absorption, implying that photoreductive activation of dioxygen does not proceed at a significant rate in aerated aqueous ethanol. Platinization results in a dramatic increase in activity with only slight build-up of negative charge. This supports the view that the noble metal serves as a “reactive sink” for electrons, thereby promoting ionosorption of dioxygen, a key initial step. Photo-oxidation of dilute aqueous ethanol proceeds through acetaldehyde and acetic acid as intermediates. Mineralization of acetic acid (acetate) is very slow and constitutes the RDS. Clear mechanistic parallels between gas- and liquid-phase ethanol photoprocesses lead to the conclusion that, depending on the availability of the chemical oxidant (a function of both experimental design and identity of the substrate molecule), photo-oxidation and photoreforming can occur in parallel. In the case of ethanol, acetaldehyde is a common intermediate in both processes, and its formation is promoted by O₂. However, other important features of this work, namely, charging of TiO₂ and growth of metal-adsorbed CO on the platinized catalyst, both under aerated conditions, raise concerns as to the efficacy of photo-oxidation processes over submerged or suspended catalysts unless due attention is given to supply (mass transfer) limitations of the oxidant in particular. On the basis of this work, it can be concluded that adventitious oxidation of ethanol in fermentation broth is extremely unlikely except by known biochemical mechanisms.

As regards the ATR-FTIR technique, as currently practiced, a number of limitations have been made evident. Probably the most serious of these is its inability to track and identify gaseous products except where speciation into the bulk liquid is possible, as with CO₂ in water. Dominance of spectral response by the bulk liquid is still a problem although a more shallow penetration depth is, in principle, achievable by using a crystal with higher refractive index, for example, Ge, albeit at the expense of sensitivity. Finally, just as in the case of DRIFTS, there remain urgent fundamental developments to make the ATR-FTIR technique more quantitative.

■ ASSOCIATED CONTENT

Supporting Information. Characterization of the catalyst, spectra of control experiments, and raw spectra of ethanol, acetaldehyde, and acetic acid photo-oxidation. This material is available free of charge via the Internet at <http://pubs.acs.org>.

■ AUTHOR INFORMATION

Corresponding Author

*E-mail: james_highfield@ices.a-star.edu.sg (J.G.H.), aszchen@ntu.edu.sg (Z.C.).

Funding Sources

The authors thank the Environment and Water Industry Program Office (EWI) under the National Research Foundation of Singapore (Grant MEWR 651/06/160) for the financial support of this work.

■ ACKNOWLEDGMENT

We are grateful to Dr. Simo Pehkonen (Masdar Institute, Abu Dhabi, UAE) for frequent consultation and Mr. Ho Yi Jie

(Victoria Junior College, Singapore) for assistance in the experiments.

■ REFERENCES

- (1) Hernandez-Alonso, M. D.; Fresno, F.; Suarez, S.; Coronado, J. M. *Energy Environ. Sci.* **2009**, *2*, 1231.
- (2) Fujishima, A.; Zhang, X. T.; Tryk, D. A. *Surf. Sci. Rep.* **2008**, *63*, 515.
- (3) Chen, X.; Mao, S. S. *Chem. Rev.* **2007**, *107*, 2891.
- (4) Fujishima, A.; Zhang, X. C. R. *Chim.* **2006**, *9*, 750.
- (5) Burgi, T.; Baiker, A. *Adv. Catal.* **2006**, *50*, 227.
- (6) McQuillan, A. J. *Adv. Mater.* **2001**, *13*, 1034.
- (7) Mojet, B. L.; Ebbesen, S. D.; Lefferts, L. *Chem. Soc. Rev.* **2010**, *39*, 4643.
- (8) Nakamura, R.; Nakato, Y. *J. Am. Chem. Soc.* **2004**, *126*, 1290.
- (9) Nakamura, R.; Imanishi, A.; Murakoshi, K.; Nakato, Y. *J. Am. Chem. Soc.* **2003**, *125*, 7443.
- (10) Araujo, P. Z.; Mendive, C. B.; Rodenas, L. A. G.; Morando, P. J.; Regazzoni, A. E.; Blesa, M. A.; Bahnemann, D. *Colloids Surf., A* **2005**, *265*, 73.
- (11) Mendive, C. B.; Bredow, T.; Blesa, M. A.; Bahnemann, D. W. *Phys. Chem. Chem. Phys.* **2006**, *8*, 3232.
- (12) Mendive, C. B.; Bahnemann, D. W.; Blesa, M. A. *Catal. Today* **2005**, *101*, 237.
- (13) Dolamic, I.; Burgi, T. *J. Phys. Chem. B* **2006**, *110*, 14898.
- (14) Dolamic, I.; Burgi, T. *J. Catal.* **2007**, *248*, 268.
- (15) Savory, D. M.; Warren, D. S.; McQuillan, A. J. *J. Phys. Chem. C* **2011**, *115*, 902.
- (16) Highfield, J. G.; Chen, M. H.; Nguyen, P. T.; Chen, Z. *Energy Environ. Sci.* **2009**, *2*, 991.
- (17) Highfield, J. G.; Chen, H. J.; Chong, C.; Chen, Z. In *Final Program & Abstract Book of The 17th International Conference on Photochemical Conversion & Storage of Solar Energy (IPS17)*, Sydney, NSW, Australia, July 27–Aug 1, 2008.
- (18) Highfield, J. G.; Geiger, F.; Uenala, E.; Schucan, T. H. In *Proceedings of The 10th World Hydrogen Energy Conference*, Cocoa Beach, Florida, June 1994; Block, D.L., Veziroglu, T.N., Eds.; International Association for Hydrogen Energy (IAHE)-Elsevier: New York, 1994; Vol. 2, p 1039.
- (19) Gong, D. G.; Subramaniam, V. P.; Highfield, J. G.; Tang, Y. X.; Lai, Y. K.; Kanhere, P. D.; Chung, Y. H.; Chen, Z. In *Final Program & Abstract Book of The 15th International Conference on TiO₂ Photocatalysis: Fundamentals and Applications*, Town & Country Resort, San Diego, California, Nov 15–18, 2010.
- (20) Yu, Z. Q.; Chuang, S. S. C. *J. Catal.* **2007**, *246*, 118.
- (21) Guzman, F.; Chuang, S. S. C. *J. Am. Chem. Soc.* **2010**, *132*, 1502.
- (22) Coronado, J. M.; Kataoka, S.; Tejedor-Tejedor, I.; Anderson, M. A. *J. Catal.* **2003**, *219*, 219.
- (23) Wu, W. C.; Chuang, C. C.; Lin, J. L. *J. Phys. Chem. B* **2000**, *104*, 8719.
- (24) Bates, S. P.; Gillan, M. J.; Kresse, G. *J. Phys. Chem. B* **1998**, *102*, 2017.
- (25) Lusvardi, V. S.; Barteau, M. A.; Farneth, W. E. *J. Catal.* **1995**, *153*, 41.
- (26) Szczepankiewicz, S. H.; Moss, J. A.; Hoffmann, M. R. *J. Phys. Chem. B* **2002**, *106*, 2922.
- (27) Szczepankiewicz, S. H.; Moss, J. A.; Hoffmann, M. R. *J. Phys. Chem. B* **2002**, *106*, 7654.
- (28) Highfield, J. G.; Pichat, P. *New J. Chem.* **1989**, *13*, 61.
- (29) Highfield, J. G.; Gratzel, M. *J. Phys. Chem.* **1988**, *92*, 464.
- (30) Vorontsov, A. V.; Dubovitskaya, V. P. *J. Catal.* **2004**, *221*, 102.
- (31) Arana, J.; Dona-Rodriguez, J. M.; Cabo, C. G. I.; Gonzalez-Diaz, O.; Herrera-Melian, J. A.; Perez-Pena, J. *Appl. Catal., B* **2004**, *53*, 221.
- (32) Pichat, P. *Catal. Today* **1994**, *19*, 313.
- (33) Pichat, P.; Mozzanega, M. N.; Disdier, J.; Herrmann, J. M. *New J. Chem.* **1982**, *6*, 559.

- (34) Gao, H. W.; Xu, W. Q.; He, H.; Shi, X. Y.; Zhang, X. L.; Tanaka, K. *Spectrochim. Acta, Part A* **2008**, *71*, 1193.
- (35) Jacobs, G.; Patterson, P. M.; Graham, U. M.; Crawford, A. C.; Dozier, A.; Davis, B. H. *J. Catal.* **2005**, *235*, 79.
- (36) Iwasita, T.; Nart, F. C.; Lopez, B.; Vielstich, W. *Electrochim. Acta* **1992**, *37*, 2361.
- (37) Hollins, P. *Surf. Sci. Rep.* **1992**, *16*, 51.
- (38) Ebbesen, S. D.; Mojet, B. L.; Lefferts, L. *J. Catal.* **2007**, *246*, 66.
- (39) Ebbesen, S. D.; Mojet, B. L.; Lefferts, L. *Langmuir* **2006**, *22*, 1079.
- (40) Ortiz-Hernandez, I.; Williams, C. T. *Langmuir* **2003**, *19*, 2956.
- (41) Highfield, J. G.; Gong, D. G.; Teo, J.; Zhong, Z.; Chen, Z., manuscript in preparation.
- (42) Alcala, R.; Mavrikakis, M.; Dumesic, J. A. *J. Catal.* **2003**, *218*, 178.
- (43) Alcala, R.; Shabaker, J. W.; Huber, G. W.; Sanchez-Castillo, M. A.; Dumesic, J. A. *J. Phys. Chem. B* **2005**, *109*, 2074.
- (44) Park, H.; Kim, K. Y.; Choi, W. *J. Phys. Chem. B* **2002**, *106*, 4775.
- (45) Howe, R. F.; Gratzel, M. *J. Phys. Chem.* **1985**, *89*, 4495.
- (46) Yoneyama, H.; Takao, Y.; Tamura, H.; Bard, A. J. *J. Phys. Chem.* **1983**, *87*, 1417.
- (47) Baltrusaitis, J.; Schuttlefield, J.; Zeitler, E.; Grassian, V. H. *Chem. Eng. J.* **2011**, *170*, 471.
- (48) Barattini, L.; Ramis, G.; Resini, C.; Busca, G.; Sisani, M.; Constantino, U. *Chem. Eng. J.* **2009**, *153*, 43.
- (49) Basagiannis, A. C.; Verykios, X. E. *Appl. Catal., A* **2006**, *308*, 182.
- (50) Medrano, J. A.; Oliva, M.; Ruiz, J.; Garcia, L.; Arauzo, J. *Int. J. Hydrogen Energy* **2008**, *33*, 4387.
- (51) Ford, D. C.; Anand, U. N.; Ye, X.; Mavrikakis, M. *Surf. Sci.* **2010**, *604*, 1565.
- (52) Tripkovic, V.; Skulason, E.; Siahrostami, S.; Norskov, J. K.; Rossmeis, J. *Electrochim. Acta* **2010**, *55*, 7975.
- (53) Zhdanov, V. P.; Kasemo, B. *Electrochem. Commun.* **2006**, *8*, 1132.
- (54) Lin, H. X. *J. Mol. Catal. A: Chem.* **1999**, *144*, 189.
- (55) Abe, R.; Takami, H.; Murakami, N.; Ohtani, B. *J. Am. Chem. Soc.* **2008**, *130*, 7780.
- (56) Liu, Q.; Bauer, J. C.; Schaak, R. E.; Lunsford, J. H. *Appl. Catal., A* **2008**, *339*, 130.